Proceedings of the 2004 IEEE
Conference on Robotics, Automation and Mechatronics
Singapore, 1-3 December, 2004

PARAMETRIC STUDY ON POLE GEOMETRY AND THERMAL EFFECTS OF A VRSM

Kok-Meng Lee*, Zhiyong Wei and Jeffry Joni
The George W. Woodruff School of Mechanical Engineering
Georgia Institute of Technology
Atlanta, GA 30332-0405
Atlanta, GA 30332-0405
*Email: kokmeng.lee@me.gatech.edu

Abstract - **The variable-reluctance spherical motor (VRSM), which offers some attractive features by combining pitch, roll, and yaw motions in a single joint, is essentially a brushless, direct-drive actuator. Unlike a multi-axes actuating mechanism where the number of electrical inputs typically equal to its number of controllable degrees of freedom, the VRSM offers a large number of distributed electrical inputs as compared to the number of controllable DOF. Since larger number of small coils is used, it not only effectively increases the surface area for heat dissipation, but also allows a small amount of current to flow through each of the coils. This distributed actuation offers an effective means to overcome heat dissipation problems commonly associated with direct-drive actuators for high torque applications. To exploit the advantages offered by this unique feature that provides a greater flexibility in design and control, a good understanding of the key parameters that could significantly influence the motor performance is essential. For this reason, we present in this paper some results of a detailed parametric study on the effects of pole geometry on the thermal and torque performance of a three degrees-of-freedom (DOF) VRSM.**

Keywords: Motor design, Stepper, spherical motor, FE analysis

I. INTRODUCTION

Motors, as energy conversion devices, are widely used in industries. One degrees-of-freedom (DOF) motors including steppers or switch -reluctance motors has reached its maturity for a long time. While these motors can provide accurate motions, the combination of these single-axis motors as multi-DOF devices are rather clumsy. Alternative designs such as ball-joint-like spherical motors capable of combining three-DOF into a single joint offer some unique advantages as compared to their counterparts.

The variable-reluctance spherical motor (VRSM) referred to in this paper has a similar structure as ball-joint-like device in [1]. As shown in Fig. 1, the structure is made up of four basic assemblies, a spherical rotor, a hollow spherical stator, a bearing system, and an orientation measurement system. The stator houses a number of electromagnets strategically distributed on the spherical surface. Similarly, the rotor consists of a number of poles made up of ferromagnetic materials or permanent magnets. The rotor poles meet at the rotor center, and the stator cores are connected by the magnetic conductor layer in the stator shell to form a magnetic circuit with the air-gaps.

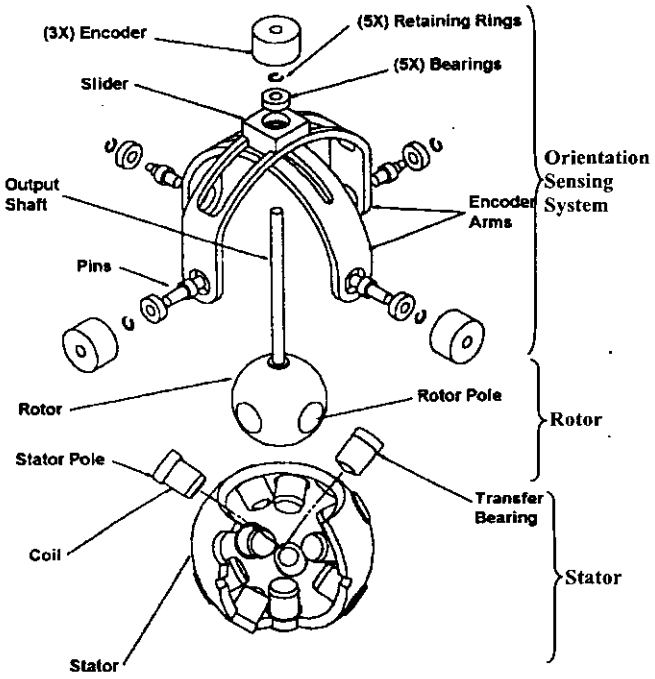

Figure 1 Exploded vie of a VRSM [1]

As shown in Fig. 1, the input power to drive the VRSM is distributed through a large amount of stator electromagnets coupled with the high coercive forces of the rare-earth permanent magnets used as rotor poles. The distributed actuation of a VRSM offers several advantages as compared to its counterparts; among these are the following: (1) Larger number of small coils can be used and thus effectively increase the surface area for heat dissipation. Moreover, it allows a small amount of current to flow through each of the coils. The heat dissipation that is proportional to the square of the current can be significantly reduced. (2) The large number of power inputs (much larger than the controllable DOF or output) implies that the inputs are highly redundant. The inverse torque model of a VRSM, which determines appropriate coil excitations for a specified torque, has multiple solutions. This feature allows an optimal control

vector to be chosen to minimize a specified cost function (for example, energy input). This characteristic significantly differs from that of a popular three-consecutive-rotational-joint wrist based on single-axis direct-drive motor or spherical motors of other types which typically have unique solutions to their inverse torque model and therefore limited the flexibility in the controller designs. (3) Perhaps, the most important advantage offered by highly redundant inputs is that ability to allow a VRSM to fail safe. In other words, the VRSM would continue to work (though sub-optimal) even if one or more individual coils fail. This beauty is attractive for applications (such as car wheels, ship propellers, helicopter rotors, transportation in underwater or outer space) where immediate attention could be gracious and/or life threatening.

The simplicity and compact design of a VRSM has motivated a number of researchers since the inception of the spherical stepper [2]. The kinematics among the poles of a VRSM was investigated in [3]. The dynamic model of a particular VRSM can be found in [1], where the torque model is a quadratic function of the current inputs to the stator coils. In [4], a similar VR spherical motor was developed with a very simple magnetic rotor assembly and coil arrangement capable of two and three DOF motions. Chirikjian and Stein [5] proposed a commutation algorithm for a spherical stepper. More recently, the interest to derive a closed-form solution to the inverse torque model has led Lee and Sosseh [6] to design a VRSM that has a linear torque-current relationship. Most of these efforts have focused on dynamic modeling and control.

To exploit the advantages offered by this unique feature that provides a greater flexibility in design and control, a good understanding of the key parameters that could significantly influence the motor performance is essential. For this reason, we present in this paper some results of a detailed parametric study on the effects of pole geometry on the thermal and torque performance of a three degrees-of-freedom (DOF) (VRSM). In [7], we have developed a numerical procedure based on computer aided design (CAD) and finite element (FE) analysis to streamline the design process and reduce development time of a new prototype.

Since the change in magnetic energy and hence the torque generated by a VRSM occurs primary in air gaps between pairs of stator electromagnets and rotor poles, we focus in this paper two design issues on the torque performance; the thermal effect and the sensitivity of pole geometries. These parametric studies provide a closed-up analysis on (and help visualize the influence of) the interacting pole-pairs. Once the optimal pole-pair geometry is pinned down, an accurate torque model for the overall VRSM can be obtained using the CAD/CAE approach given in [7].

The remainder of this paper is organized as follows: Section II examines the thermal effects of the stator coil. Next, we investigate the sensitivity of the rotor geometry for a given coil design on the torque performance in Section III. Once the design influences of the rotor poles and stator coils are well understood, the effects of the pole/coil distribution on the overall control system are then evaluated.

II. THERMAL EFFECTS

A thermal model that solves the three-dimensional heat conduction equation has been built with ANSYS for analyzing the temperature field of the stator coils so that the thermal effects on different motor designs can be compared. Due to the symmetry, only 1/N fraction of the stator (2 coils) is included in the computation domain. Along the planes of symmetry, adiabatic conditions are applied. In the following comparisons, part or all the surfaces of the coils are exposed to the ambient air.

A. Thermal Model of a Coil

The coil is modeled as a uniform heat source, which can be calculated from the time-average current input and the electrical resistance of the wire, with an apparent conductivity that accounts for the thermal resistance due to the air space in the copper coil. Geometrically, the coil is modeled as a hollow cylinder.

In order to provide a reasonable approximation, we compute the time-average currents in 5 stator coils as the rotor spins one complete rotation. Fig. 1 shows a typical current history of two stator coils captured for 0.5 second. The RMS values of the five current, which are used as measures of power dissipation, are almost the same:

1.4347 1.4378 1.4472 1.4461 1.4376

Thus, a single value is used for the current of all the stator coils in the following discussion for comparing designs.

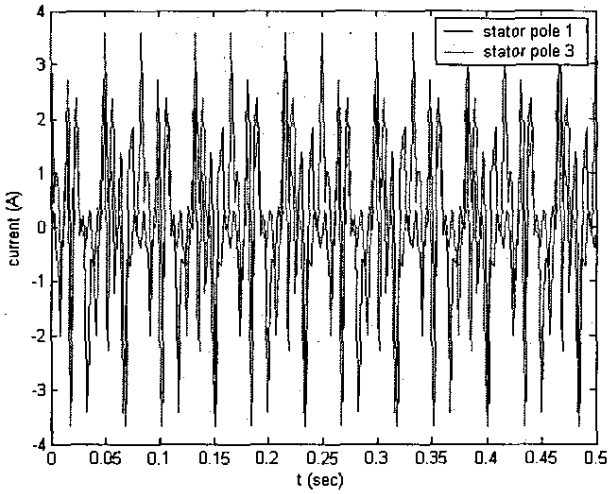

Figure 3 Current history in stator coils (1 and 3)

B. Effect of Stator Coil Designs

We consider two different stator-coil configurations as summarized in Table 1, where

- n = number of stator coils;
- ID_s and OD_s are the inside and outside diameters of the stator shell (in inches)
- ID_c, OD_c and L are the inside and outside diameters and the length of the stator coil (in inches);

N, I and Q are the number of turns, current (in Ampere) and the power dissipation (W/coil) of the stator coil. The ampere-turn (NI) is kept almost the same.

Other values of the parameters are given in Table 2.

TABLE I DIMENSIONS AND PARAMETERS OF THE COILS

n	ID_s	OD_s	ID_c	OD_c	L	N	I	Q
10	6	6.76	0.375	1	1	806	1.5	11.52
24	3.46	4.46	0.2	0.5	0.7	720	1.5	14.3

TABLE 2 SIMULATION PARAMETERS AND VALUES

Copper wire resistivity: 1.724×10^{-8} ohm-m (at 20°C).
Temperature coefficient of copper: $\alpha = 0.005$ 1/°C and $\Delta R = \alpha R_0 \Delta T$.
Apparent conductivity of coil = 4.15 W/mK,
Air natural convection coefficient = 11.5W/m^{2}K
Temperature of the base (as a heat sink) =27°C or 80°F

Effects of materials

We compare the thermal performance of three designs that use different materials and wire size for the stator coils for a VRSM with n=10 coils:

Design #1: stator shell is made of iron and the cores are of Delrin plastic; and

Design #2: both the stator shell and the cores are made of aluminum.

Design #3: Same as Design #2 except a smaller wire size was used.

The temperature distributions computed using ANSYS for *Designs #1* and *#2* are compared in Fig. 4. In both designs, heat generated by the coil is cooled by natural convection of the surrounding air, and conduction to the iron shell via the copper coils. Results of the comparison are briefly summarized as follows:

- The maximum temperature of *Design #2* is 42% of that in *Design #1*.
- *Design #1* relies on the copper coils to conduct heat to the iron shell since the plastic core does conduct heat effectively. This results in an accumulation of heat in the inner head of the coil as shown in Fig. 4(a).
- Since both the aluminum core and the copper coil conduct heat effectively to the state shell, the maximum temperature of *Design #2* occurs around the outer surface of the stator coil as shown in Fig. 4(b), where heat is dissipated by means of natural convection through a small area as in *Design #1*.
- Fig. 4(c) shows the temperature distribution computed for *Design #3* with a small wire diameter of 0.127mm, which is similar to Fig. 4(b). The use of a smaller wire diameter tends to increase the coil resistance but on the other hand, requires a shorter length of coil wire for a same number of turns and core diameter. This presents an interesting design tradeoff.

Effect of heat transfer modes

One effective way to further lower the coil temperature is to increase the surface contact between the copper coil and the stator shell. To simulate the effect of force convection, the base is increased by 19mm (0.75 inch) in height and the heat transfer coefficient h is increased by a factor of two. Three 24-coil configurations are compared in Fig. 5 and Table 3:

Design #4: half of the coil is embedded in the shell;

Design #5: the coil is embedded in the shell, and

Design #6: Design #4 but with forced convection.

As compared between Figs. 5(a) and 5(b), the maximum temperature can be reduced as much as 30% simply by embedding the remainder of the coil. Figs. 5(a) and 5(c), which compare *Design #3* with and without force convection, show that the maximum temperature is reduced by only 5°C (or 6%).

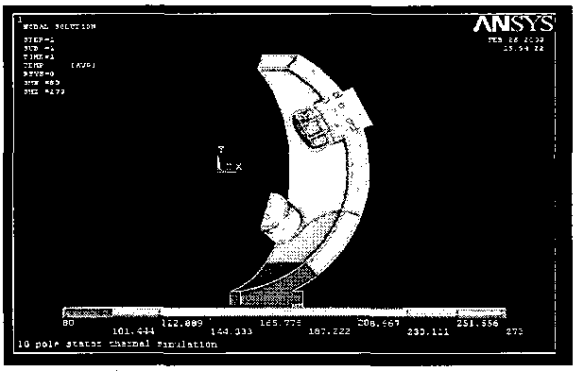

(a) Design #1 (Tmax=133°C or 273 °F), OD_w=0.381mm

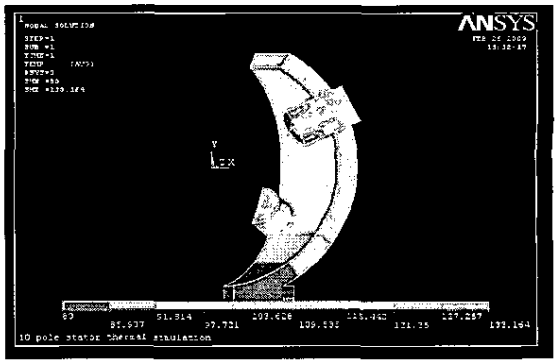

(b) Design #2 with OD_w=0.381mm (T_{max} = 56°C or 133°F)

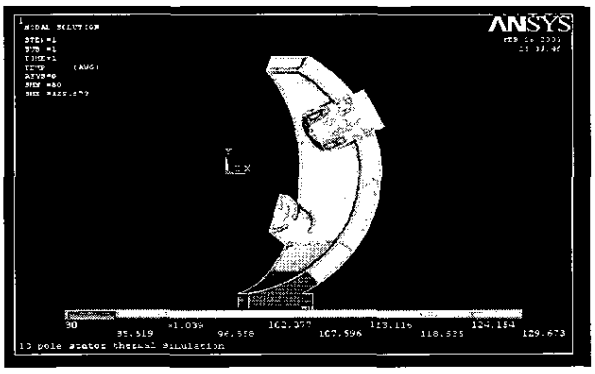

(c) Design #2 with OD_w=0.127mm (T_{max} = 54°C or 130°F)

Figure 4 Temperature Distribution (10-coil design)

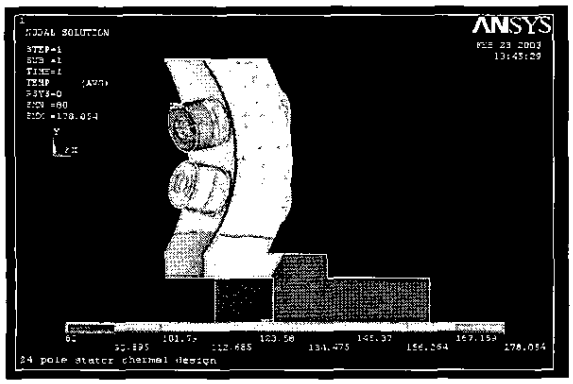

(a) *Design* #3 with NC, (Tmax = 81°C or 178 °F)

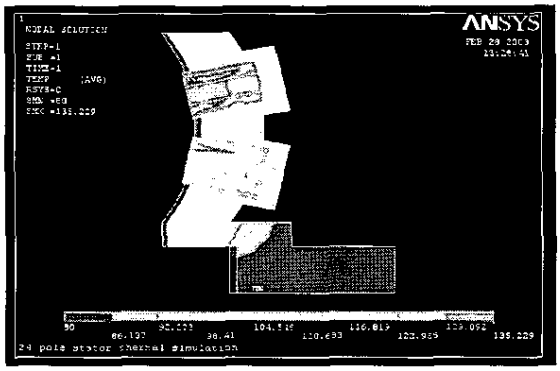

(b) *Design #4,* (Tmax = 57°C or 135 °F), NC

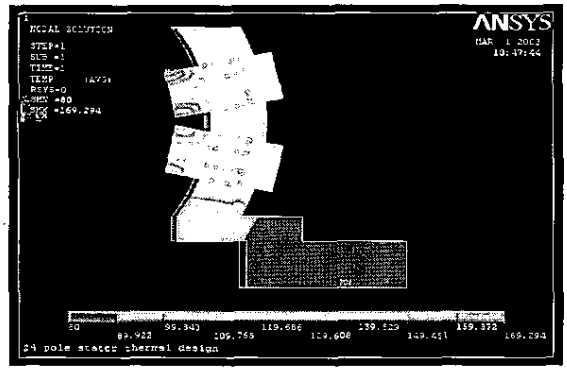

(c) *Design #3* with FC, (Tmax = 76°C or 169 °F),

Figure 5 Effect of Stator Design
(NC= natural Convection, FC= Force convection)

TABLE 3 COMPARISON OF DIFFERENT DESIGNS

Design	Coils	NI	Convection	OD_w (in)	Tmax (°C)
#1	10	1209	Natural Convection	0.016	133
#2					56
#3				0.005	54
#4	24	1080		0.0097	81
#5					57
#6			Forced Conv.		76

III. EFFECTS OF ROTOR POLE DESIGN

For a given thermal specification on the design of the electromagnet, the torque performance depends on the geometry of pole-pair and the magnetic flux path. To study the effects of these parameters, an ANSYS electromagnetic model has been built to compare the torques of different designs. The Maxwell's equation is solved using the scalar potential formulation. The virtual work method is used to calculate the force distribution on the rotor, which is then integrated to obtain the torque. The detailed models and the solution method can be found in [6] and [7].

We consider two interacting pairs, where the rotor pole is rotated with respect to an electromagnet wound on a non-ferromagnetic core. As in [6], the FE analysis is performed for two opposite interacting pairs of the rotor magnets and stator coils as shown in Fig. 6. Unlike the prototype in [6] where six equally spaced rotor magnets are used, we consider here a design where the number of equally spaced rotor magnets is a multiple of four; the primary difference is that the magnetization axes of the diametrically opposite pair for the six-magnet design is pointing in the same direction whereas the pair for the 4X-magnet design is pointing in the opposite direction as illustrated in Fig. 6. Four different rotor pole designs are compared in Table 3 and as shown in Fig. 6, a thin layer of iron cap is added to the rotor magnet to form a spherical rotor surface. Since the iron permeability is nearly infinite as compared to air, the iron surface is assumed to be equi-potential.

TABLE 3: POLE CONFIGURATIONS

Stator coil geometry:
Inside diameter: 9.525mm or 0.375inch
Outside diameter: 19.05mm or 0.75inch
Length of coil: 25.4mm or 1 inch
Number of turns: 1050 turns; Current: 4A

Rotor pole geometry:
Magnet: axially magnetized cylindrical NeFeB magnets

Pole designs	Magnet geometry mm (inch)		Iron cap diameter mm (inch)
	diameter	Length	
PD-A	12.5 (0.5)	12.5 (0.5)	19.0 (0.75)
PD-B			12.5 (0.5)
PD-C	19.0 (0.75)	5.59(0.22)	19.0 (0.75)
PD-D			

Air gap between stator and rotor poles: 0.75mm or 0.03inch

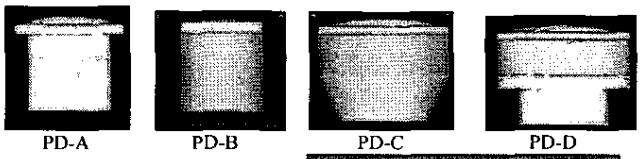

FE analysis based on two diametrically opposite pairs of poles.→

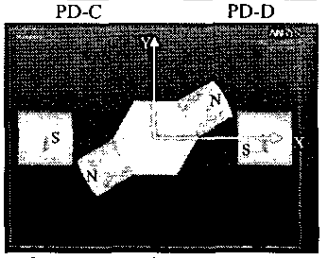

Figure 6 Comparison of rotor geometries

Fig. 7 compares two different (ferrous and non-ferrous) materials used for the center block on which the rotor magnets are mounted. The result shows that the effect of the materials (iron vs. aluminum) on the torque curve is relatively small. This is somewhat expected since two interacting pairs are essentially independent of each other due to the magnetization axes of the rotor magnets.

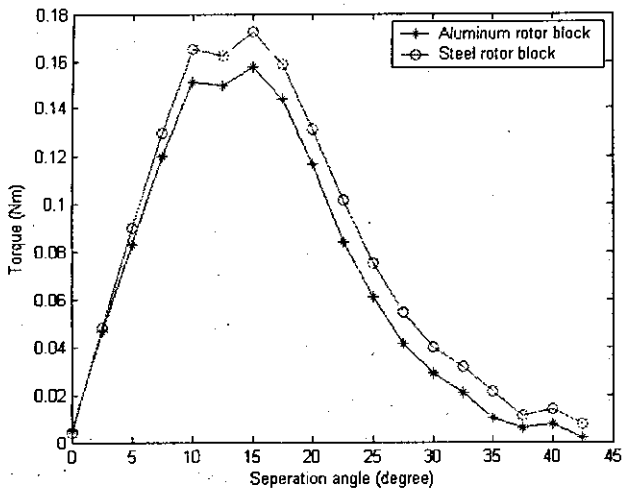

Figure 7 Effect of rotor center-block material (PD-B)

Fig. 8 compares the torque curves of four different rotor designs as a function of separation angle with respect to the stator electromagnet, all of which are mounted on aluminum center block. Table 4 summarizes the maximum torques and the locations at which the maximum torques occur for the four rotor pole designs

TABLE 4: COMPARISON OF MAXIMUM TORQUES

Pole designs	Max. torque (Nm)	Location of max. torque (degrees)
PD-A	0.10	18
PD-B	0.16	12
PD-C	0.14	15
PD-D	0.24	15

The following observations can be made from the results shown in Fig. 8:

(1) The rotor cap of PD-A was designed to match the outside diameter of the stator coil, which is 25% larger than that of PD-B designed to match the diameter of the rotor magnet. The maximum torque occurs at a larger separation angle in PD-A as expected since its rotor cap has a larger diameter. However, the maximum torque generated by PD-B is about 60% higher of that generated by PD-A, and most part of the torque curve of PD-B is much higher than that of PD-B. The overhanging portion of the rotor cap results in significantly large flux leakages (or fluxes that do not flow cross the air gap.)

(2) The two different magnets shown in Table 3 have a same volume but different aspect ratios (height-to-diameter). In addition, the overall height of the rotor is kept at a constant by adding iron to the base of the magnet so that the same air gap spacing between the stator/rotor pole-pair can be maintained. As shown in Table 4 and Fig. 8, a small aspect ratio of the magnet can significantly increase the magnitude of the generated torque as much as 50% as compared between PD-B and PD-D; provided that the rotor pole is designed to prevent flux leakages around the magnet.

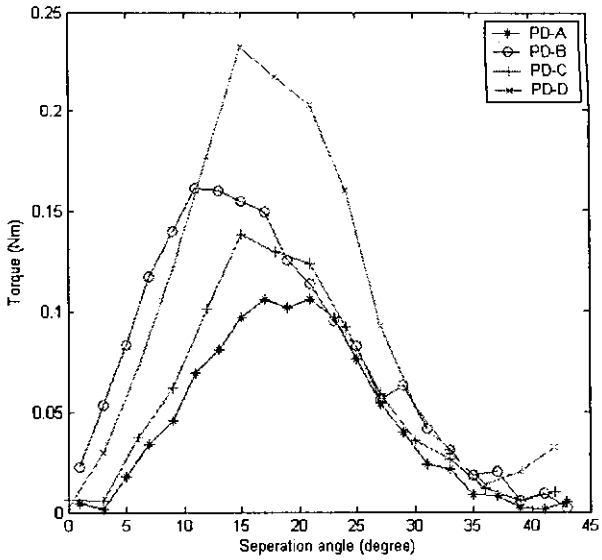

Figure 8 Effect of rotor pole geometry

VI. EFFECTS OF POLE/COILS DISTRIBUTION

One of the design tradeoffs for a given motor size is the number of rotor magnets and stator coils that can be distributed on the surface area. To study this effect, we compare two configurations shown in Table 5, where the 10-coil/6-PM design has based on (Lee and Sosseh, 2002).

TABLE 5: PARAMETERS OF TWO DESIGN CONFIGURATIONS

	10-coil/6-PM Lee & Sosseh, 2002	**24-coil/16-PM design**
Rotor PD-B pole, mm (inch)		
Diameter	19.0 (0.75)	12.5 (0.5)
Length	19.0 (0.75)	12.5 (0.5)
Location from xy plane	0°	±20° (8 each)
Stator coil, mm (inch)		
Inside diameter	9.5 (0.375)	9.5 (0.375)
Outside diameter	25.4 (1.00)	19.0 (0.75)
Length	25.4 (1.00)	25.4 (1.00)
Wire diameter	0.381mm	0.127mm
Ampere, turns	4A, 1000 turns	4A, 1050 turns
Location from XY plane	±26° (5 each*)	±26° (12 each)

* The coils are placed at the vertices of an icosahedrons without and top and bottom points.

Fig. 9 compares the torque curves obtained using ANSYS for two diametrically interacting pairs of the rotor magnets and stator coils. While the magnet volume ratio between the 10-6 design to the 24-16 design is about 3.5 but the corresponding maximum torque ratio is only nearly 2. With the torque curves given in Fugue 10, we compare their responses to a step change of (θ_x=30°, θ_y=0°, θ_z=60°) using the back-stepping control algorithm described in (Lee and Sosseh, 2002). As compared in Figs. 10 and 11, the response of the 24-16 design not only has a much lower overshoot with a shorter response time, but also dissipates a lot less heat. A close examination of the results shows that the maximum desire input current for the 10-6 design is well beyond the saturation limit of 4A. The large distribution of the poles/coils in the 24-16 design results in a relative lower maximum current of only 2.66A.

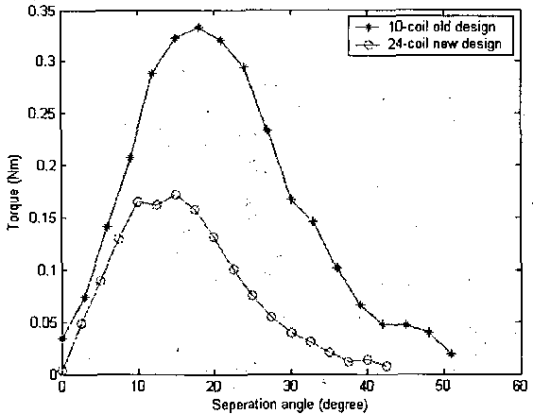

Figure 9 Comparison of torque curve (10-6 vs.24-16)

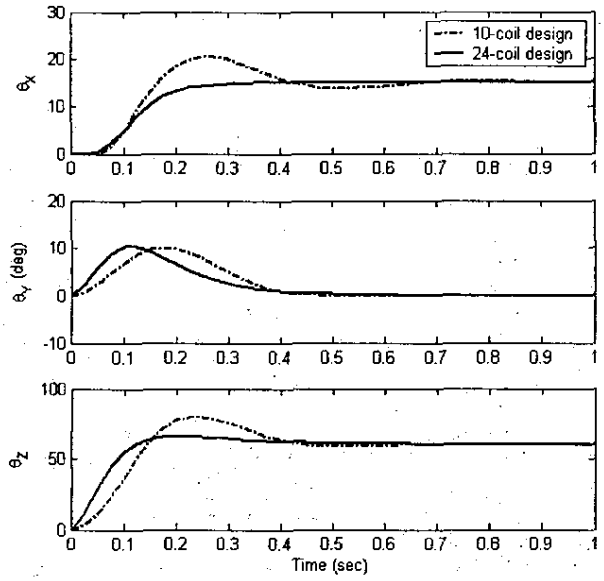

Figure 10 Comparison of step responses (10-6 vs. 24-16)

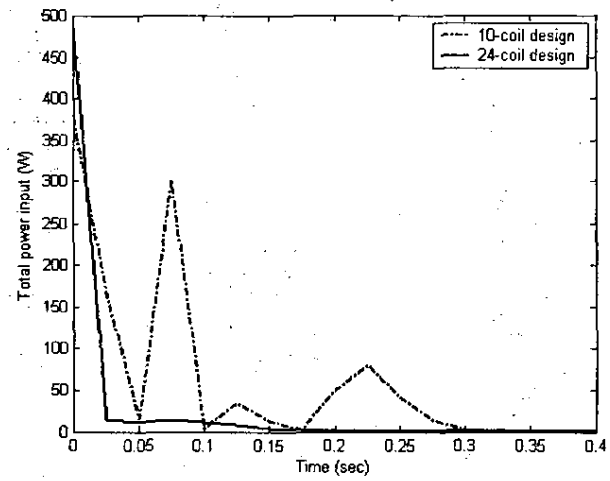

Figure 11 Total transient power inputs (10-6 vs.24-16)

V. CONCLUSIONS

We have presented a detailed parametric study highlighting the thermal effects of the stator coil design, the sensitivity of rotor geometries on the torque performance, and the pole/coil distribution on the step responses of a three degrees-of-freedom (DOF) variable-reluctance spherical motor (VRSM).

By comparing different heat transfer modes for cooling, we have shown that a well-designed conduction cooling can effectively reduce the maximum temperature of the electromagnet. We have also demonstrated that a large distribution of rotor poles and stator coils effectively reduces heat dissipation, overshoot and response time during the transient.

We have also showed that the magnitude of the generated torque can be significantly increased by using a small height-to-diameter ratio provided that the overall rotor pole is designed to_avoid potential_flux leakages. These parametric studies provide a closed-up analysis on (and help visualize the influence of) the interacting pole-pairs for improving the torque performance. Once the optimal pole-pair geometry is pinned down, a more accurate torque model for the overall VRSM can be experimentally verified.

REFERENCES

[1]. Lee, K-M., Roth, R., & Z. Zhou, (1996). Dynamic Modeling and Control of a Ball-joint-like VR Spherical Motor. ASME J. of Dyn. Sys., Meas. and Control, vol. 118, no. 1, pp. 29-40.

[2]. Lee, K.-M. and C.-K.Kwan, 1991" Design Concept Development of a Spherical Stepper Wrist Motor," IEEE Trans. on Robotics and Automation, V.7, No.1, pp. 175-181.

[3]. Lee, K.-M. and Pei, J., 1991, "Kinematic Analysis of a Three-DOF Spherical Wrist Actuator," Proc. of the 5th Int. Conf. on Advanced Robotics, Pisa, Italy, June 20-22.

[4]. Wang, J., Jewel, G., & Howe, D. (1997). Modeling of a Novel Spherical Permanent Magnet Actuator. Proc. ICRA'97, Albuquerque, New Mexico, pp. 1190-1195.

[5]. Chirikjian, G. S., & D.Stein, (1999). Kinematic Design and Commutation of a Spherical Stepper Motor. IEEE/ASME Trans. on Mechatronics, vol. 4, n 4, Piscataway, New Jersey, pp. 342-353.

[6]. Lee, K.-M. and R. A. Sosseh, 2002 "Effects of the Torque Model on the Control of a VR Spherical Motor," *Proc. of the 2nd IFAC Conference on Mechatronic Systems*, Berkeley, California, December 9-11, 2002. pp. 37-42. Also in *IFAC Journal of Control Engineering Practice*, Vol. 12/11, pp. 1437-1449.

[7]. Lee, K.-M. J. Joni, and H Son, 2004 "Design Method for Prototyping a Cost-Effective Variable-Reluctance Spherical Motor (VRSM), IEEE Conference on Robotics, Automation and Mechatronics (RAM), 1-3 December, Singapore.